

Wave propagation in a non-linear quasiperiodic Kronig-Penney lattice

This article has been downloaded from IOPscience. Please scroll down to see the full text article.

1994 J. Phys.: Condens. Matter 6 7741

(<http://iopscience.iop.org/0953-8984/6/38/012>)

View [the table of contents for this issue](#), or go to the [journal homepage](#) for more

Download details:

IP Address: 171.66.16.151

The article was downloaded on 12/05/2010 at 20:34

Please note that [terms and conditions apply](#).

Wave propagation in a non-linear quasiperiodic Kronig–Penney lattice

N Sun†, D Hennig†‡, M I Molina† and G P Tsironis†

† Computational Physics Laboratory, Department of Physics, University of North Texas, Denton, TX 76203, USA

‡ Freie Universität Berlin, Fachbereich Physik, Institut für Theoretische Physik, Arnimallee 14, 14195 Berlin, Germany

Received 4 May 1994, in final form 4 July 1994

Abstract. We study the transmission problem for electrons in an alternately linear–non-linear medium using a quasiperiodic Kronig–Penney model whose variance in spatial locations obeys the Fibonacci rules. We find that for waves with low intensity and long wavelength, non-linearity enhances the lattice transparency.

1. Introduction

With the advances of new technology and experimental techniques in solid state, laser optics and material science, more and more artificial materials with special structures and properties have been invented, such as alternating metal–semiconductor or semiconductor–insulator layers, and three-dimensional dielectric inhomogeneous lattices. Examples of the advances in new experimental techniques are molecular-beam epitaxy (MBE) and metallorganic vapour-phase epitaxy (MOVPE), and more sophisticated electronic and optic materials with high qualities and peculiar structures and properties will be fabricated with advanced technology. During the last decade, there has been increasing interest in the study of localization and transmission of electrons, phonons, magnetons and other quasiparticles in the superlattices of layered structures [1–4]; in the last few years, the activities have expanded to include photonic band structures in a dielectric lattice, which bears similarities to the electronic band structures in many aspects [5–10].

Recently, there has been theoretical discussion concerning the role that non-linearity might play in such multilayered structures [11, 12]. It has been shown that there are some interesting properties in a quasiperiodic superlattice when non-linearity is introduced into the quasiperiodic models, e.g. soliton-like states may exist [13], and transmission regions can be enhanced by non-linearities [14]. In particular, a Kronig–Penney model has been studied with discontinuous potentials whose bivalued strengths are arranged in a quasiperiodic sequence [14]. It turned out that while quasiperiodicity destroys the transparency of a linear superlattice for small wave numbers (long waves), non-linearity enhances it in a self-trapped mechanism. We study a similar model but with the *sequential intersite distance* being quasiperiodic. We will consider mainly the electronic wave for positive potentials but will discuss the results for negative (attractive) potentials, and compare them with the transmission of electromagnetic waves. Finally, we will explain the enhancement of transparency of the quasiperiodic chain for low-intensity long waves.

In section 2, we will give a general description of the model that will be considered. In section 3 we will discuss the propagation of plane waves and the algorithm for numerical calculations; we will also analyse and compare the transmission properties of the linear and non-linear models. Section 4 is devoted to the analysis of long-wavelength waves and their transmission at low intensity. A summary and a concluding discussion are given in section 5.

2. Non-linear Kronig–Penney model

We consider the general Kronig–Penney equation

$$-\frac{d^2\psi(z)}{dz^2} + \sum_{n=1}^N \lambda \delta(z - z_n) g(z) \psi(z) = E \psi(z) \quad (1)$$

where for the linear (L), non-linear (NL) and general non-linear (GNL) models we define

$$g(z) = \begin{cases} 1 & \text{L} \\ |\psi(z)|^2 & \text{NL} \\ \alpha_0 + \alpha_1 |\psi(z)|^2 & \text{GNL} \end{cases}$$

where (α_0, α_1) are real numbers. In equation (1), $\psi(z)$ represents an electronic wavefunction or, in a slightly modified form, is the complex amplitude of an electromagnetic plane wave with energy (or frequency) E along direction z [15, 16], and λ is a coefficient which could be used to represent variation in potential height [14]. But we keep $\lambda = 1$ in this paper. The δ functions represent the defects in a quasi-one-dimensional conductor (e.g. conducting polymers) or semiconductor chain, or small non-linear dielectric regions that are quasiperiodically embedded in a linear dielectric medium. These non-linear regions are assumed to be much smaller than the distance between adjacent linear ones. The intersite distances $d_n = z_n - z_{n-1}$ are assumed to be quasiperiodic and follow the Fibonacci sequence. There are two values of d_n , $d_n = 1$ or $d_n = a > 1$ resulting from the actual location of z_n which is determined by the rule

$$z_n = n + (a - 1) \left[\frac{n + 1}{\omega} \right]$$

with $\omega = (1 + \sqrt{5})/2$ being the golden mean and the bracket $[]$ denoting the integer part. When the intersite distance d_n is a constant, it can be shown that finding the solution of equation (1) is equivalent to solving the problem of a non-linear tight-binding model [17, 18], but this is no longer true for the quasiperiodic non-linear lattices which are being studied here.

In the following sections, we will be primarily working on the non-linear model, and the formulation can be easily extended to include the GNL model. The effects and results of the GNL model will be included in the figures and given brief discussions and comparisons with the linear model.

3. Transmission of plane waves

In the interval between z_n and z_{n+1} the solution of the Schrödinger equation can be written as

$$\psi_n(z) = A_n e^{ik(z-z_n)} + B_n e^{-ik(z-z_n)} \quad (2)$$

where k is the wave vector. We want to establish a non-linear transformation, connecting the amplitudes (A_n, B_n) and (A_{n-1}, B_{n-1}) on adjacent sides of the δ -function potential, such that

$$\begin{pmatrix} A_n \\ B_n \end{pmatrix} = P_n \begin{pmatrix} A_{n-1} \\ B_{n-1} \end{pmatrix} \tag{3}$$

where P_n is the symbolic non-linear operator, or a non-linear map which projects one set of complex numbers to another. The transformation is generally not symplectic, although the transformations on (ψ_n, ψ_n') are. This is because unlike (ψ_n, ψ_n') , (A_n, B_n) are not canonical variables. Similarly as in the linear Kronig–Penney problem, straightforward manipulations, considering the continuity of the wave functions and discontinuity of their derivatives at the boundary near the potential, lead to a (non-linear) Poincaré map for A_n and B_n . In order to simplify notations we define first for the amplitudes

$$\begin{pmatrix} \bar{A}_{n-1} \\ \bar{B}_{n-1} \end{pmatrix} = \begin{pmatrix} A_{n-1}e^{ikd_n} \\ B_{n-1}e^{-ikd_n} \end{pmatrix}$$

where $d_n = z_n - z_{n-1}$ is the distance between two consecutive potentials. We obtain the following Poincaré map for the non-linear model:

$$\begin{pmatrix} A_n \\ B_n \end{pmatrix} = P_n \begin{pmatrix} A_{n-1} \\ B_{n-1} \end{pmatrix} = \begin{pmatrix} \bar{A}_{n-1} - i(\lambda/2k)|\bar{A}_{n-1} + \bar{B}_{n-1}|^2(\bar{A}_{n-1} + \bar{B}_{n-1}) \\ \bar{B}_{n-1} + i(\lambda/2k)|\bar{A}_{n-1} + \bar{B}_{n-1}|^2(\bar{A}_{n-1} + \bar{B}_{n-1}) \end{pmatrix} \tag{4}$$

and for the inverse transformation, we have the following:

$$\begin{pmatrix} A_{n-1} \\ B_{n-1} \end{pmatrix} = P_n^{-1} \begin{pmatrix} A_n \\ B_n \end{pmatrix} = \begin{pmatrix} [A_n + i(\lambda/2k)|A_n + B_n|^2(A_n + B_n)]e^{-ikd_n} \\ [B_n - i(\lambda/2k)|A_n + B_n|^2(A_n + B_n)]e^{ikd_n} \end{pmatrix}.$$

For a finite chain of N sites, the final coefficients of the wave function are

$$\begin{pmatrix} A_N \\ B_N \end{pmatrix} = \prod_{n=N}^1 P_n \begin{pmatrix} A_0 \\ B_0 \end{pmatrix}. \tag{5}$$

Equation (5) is a non-linear map; for various initial conditions it describes waves injected initially from the left, and propagating towards the right side of the chain. Therefore, equation (5) or its inverse form can be used to study the transmission properties of the lattice by assuming a given pair of either (A_0, B_0) or (A_n, B_n) . The results are analysed to obtain the transmission properties of the lattice. In figure 1, we show the transmission behaviour in the $|R_0| - k$ parameter plane, where $|R_0|$ is the amplitude of the injected wave for the linear Kronig–Penney Fibonacci (figure 1(a)), the non-linear (figure 1(b)), and the GNL models (figure 1(c)). Dark regions represent gaps in the wave propagation whereas the transmitting regions are white. In the linear case, we have the typical band structure resulting from quasiperiodicity [19]. We note that the effect of non-linearity substantially alters this structure resulting in enhanced propagation for small initial intensities. The lattice is transparent for essentially all wavenumbers k at low intensities. In particular, the dominant linear gap for $k \lesssim 2$ is reduced drastically. The boundary between the gap and the transmission regions for small k is almost linear due to the self-trapping effect of the non-linear medium for the long wave (section 4). In the higher-intensity region, on the other hand, the forbidden lines seem to coalesce together to form well defined non-linear gaps that are interrupted periodically by propagating resonance-like zones. The latter occur for k -values that are multiples of π ; for these wavenumbers the non-linear term is effectively cancelled leading to perfect propagation.

For the GNL model, the results depend on the choice of α values. We find that, when $\alpha_1 < 0$, the transparency is enhanced as compared with the corresponding linear case; otherwise, it is reduced.

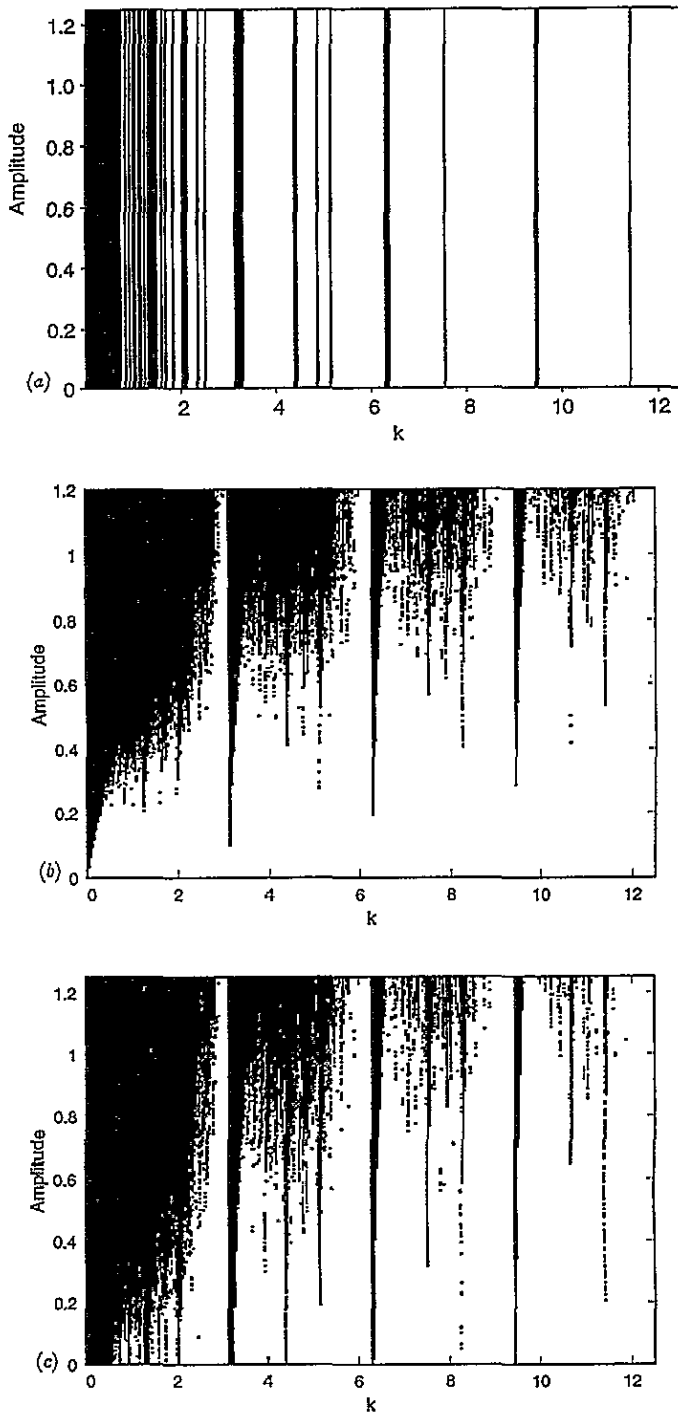


Figure 1. Non-transmitting (black) and transmitting (white) regions for a Fibonacci lattice of length $N = 987$ corresponding to the Fibonacci number F_{16} . (a) The linear model. (b) The non-linear model. Gap regions have disappeared for low-intensity waves with small wave number. The boundary between gap and extended states for small k is a straight line. (c) The GNL model with $\alpha_0 = \alpha_1 = 0.5$. It shows mixed results for transmission.

To analyse further the effects of non-linearity in the model we calculate the transmission function $t = |T|^2/|R_0|^2$, where T is the transmitted amplitude at the end of the chain and $R_0 = |\psi_0|$ is the incident wave amplitude at the beginning of the chain. In figure 2, we plot the transmission function against wavenumber k with incident wave amplitude $R_0 = 0.2$. As expected, the linear case shows (figure 2(a)) that the transmission or gap does not depend on the amplitude, and a large gap area exists for small k ; the non-linear model (figure 2(b)) demonstrates almost a total transparency for the entire spectrum of k , because the dependence of the interaction between the wave and the medium on the wave amplitude makes it easier for waves with relatively small amplitudes to transmit. The picture becomes more complicated when both linear and non-linear interactions are included. An example is given in figure 2(c).

In figure 3, we plot transmission as a function of the chain length for the linear Fibonacci Kronig–Penney case (figure 3(a)) and the non-linear ones (figure 3(b) and (c)) for $k = 0.2350$. In the linear case the transmission drops exponentially whereas in the non-linear case we have windows with perfect transmissivity. In the latter system t remains very close to unity. Fractal structures are present for both linear and non-linear lattices due to the quasiperiodicity of the lattices. In figure 4, the boundary separating transmitting (white) from non-transmitting (grey) regions also shows a fractal structure, especially at large k -values. Similar fractal behaviour has been reported by Delyon *et al* for a related model [20].

4. Low-intensity transparency for long waves

In this section we use the long-wave approximation and show in detail why transparency is enhanced for low-intensity waves. With long waves, $kd_n \ll 1$, $\exp(\pm ikd_n) \simeq 1 \pm ikd_n$. We will be able to solve the non-linear equations in (4) by taking the long-wave approximation. Let us define

$$\psi_n \equiv \psi_n(z_n) = A_n + B_n \quad \xi_n = B_n - A_n. \tag{6}$$

According to equation (2), ψ_n is the wavefunction at site n , whereas ξ_n is only a temporary variable for algebraic convenience. Then equation (4) can be expanded and regrouped to form ψ_n and ξ_n , and, by keeping only the first-order terms, it is easy to see that

$$\begin{cases} \psi_n &= \psi_{n-1} - ikd_n \xi_{n-1} \\ \xi_n &= \frac{\xi_{n-1} - ikd_n \psi_n + i\lambda}{k|\psi_n|^2 \psi_n} \end{cases} \tag{7}$$

Taking the continuum limit as $k \rightarrow 0$, or more appropriately, $k^{-1} \gg d_n$, equation (7) becomes a pair of coupled differential equations.

$$\begin{cases} \frac{d\psi(n)}{dn} &= -ik\xi(n) \\ \frac{d\xi(n)}{dn} &= -ik\psi(n) + i\frac{\lambda}{kd} |\psi(n)|^2 \psi(n) \end{cases} \tag{8}$$

where we have replaced d_n with its average d . Substituting the second equation in equation (8) into the first one after differentiation, we obtain the following second-order differential wave equation:

$$\ddot{\psi}(n) = -k^2 \psi(n) + \frac{\lambda}{d} |\psi(n)|^2 \psi(n). \tag{9}$$

We can distinguish three cases.

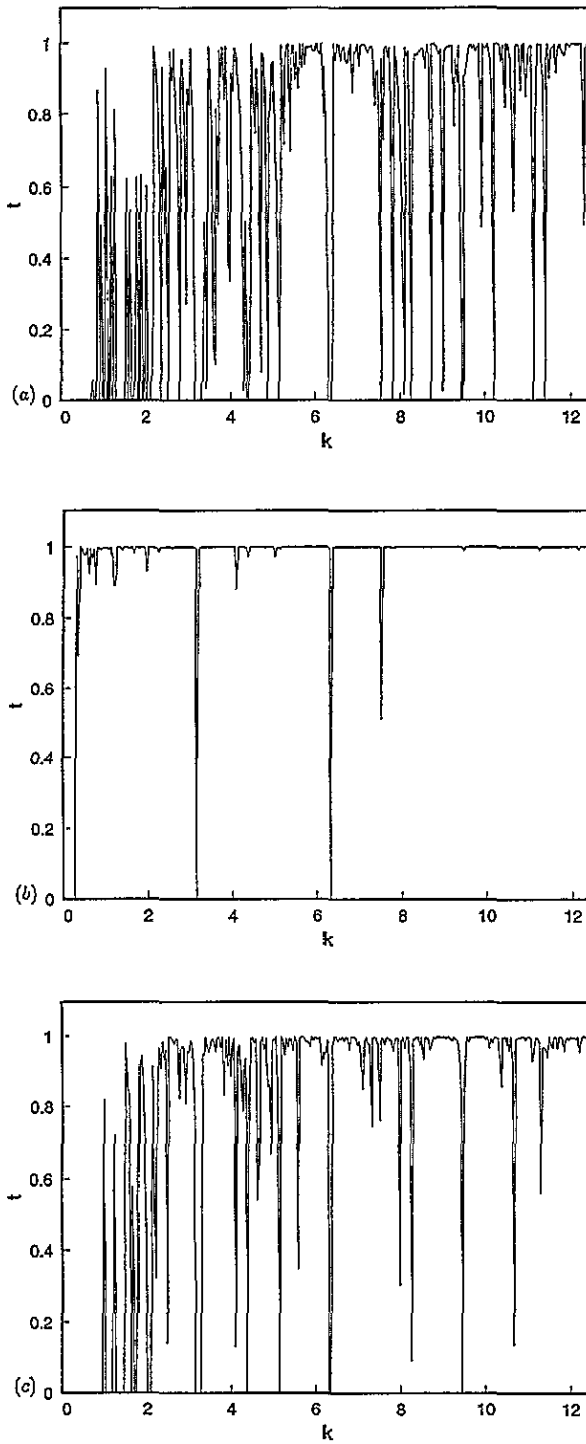


Figure 2. Transmission against wavenumber k . The initial wave amplitude is 0.2 and the length of the Fibonacci chain $N = 987$. (a) The linear Kronig–Penney model. (b) The non-linear model. It shows that transmission is enhanced for almost the whole spectrum of k at low intensity. (c) The GNL model with $\alpha_0 = \alpha_1 = 0.5$.

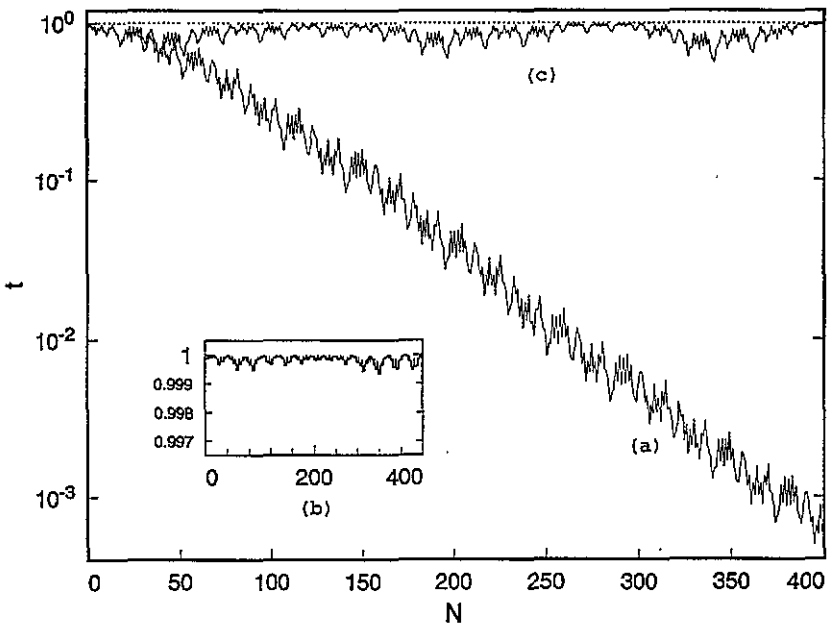


Figure 3. Transmission against chain length. The wave amplitude is 0.2, and $k = 0.23590$. (a) The linear model, which shows the exponential decay of the transmission function t . (b) The non-linear model, which appears to be a straight line at $t = 1$ in the main figure (dotted line), but actually has its own fractal structure, as shown in the inset. (c) The general non-linear model.

4.1. The linear case

Replacing $|\psi|^2$ with unity in equation (9) yields the linear equation

$$\ddot{\psi} = -\left(k^2 - \frac{\lambda}{d}\right)\psi \equiv -\sigma^2\psi.$$

When $\sigma^2 < 0$, wavenumber k is small, there are only exponential solutions, which results in a localized state. Roughly speaking, extended states will happen when k is of the order of $k_e \equiv \sqrt{\lambda/d}$. For example, in the previous section, we used $\lambda = 1$, $d = 1.618$, so that $k_e = 0.786$, and this result is consistent with figure 1(a).

4.2. The non-linear case

Let $\psi(n) = \psi_0 \exp[i\sigma n]$ be a solution of equation (9), then we find

$$\sigma^2 = k^2 - \frac{\lambda}{d}|\psi_0|^2. \tag{10}$$

Unlike the linear case, whether σ is real or imaginary now depends on the intensity of the wave $|\psi_0|$. As long as $|\psi_0| < \sqrt{\lambda/d}k$, there will be propagating waves and hence extended states. Let $\sigma = 0$, we have

$$|\psi_0| = \sqrt{\lambda/d}k. \tag{11}$$

Equation (11) represents the boundary that separates the gap state from the propagating state for very small k . Figure 4 shows the result from numerical calculation which agrees with equation (11) for small k . We used $\lambda = 1$, and the average intersite distance $d = 1.618$.

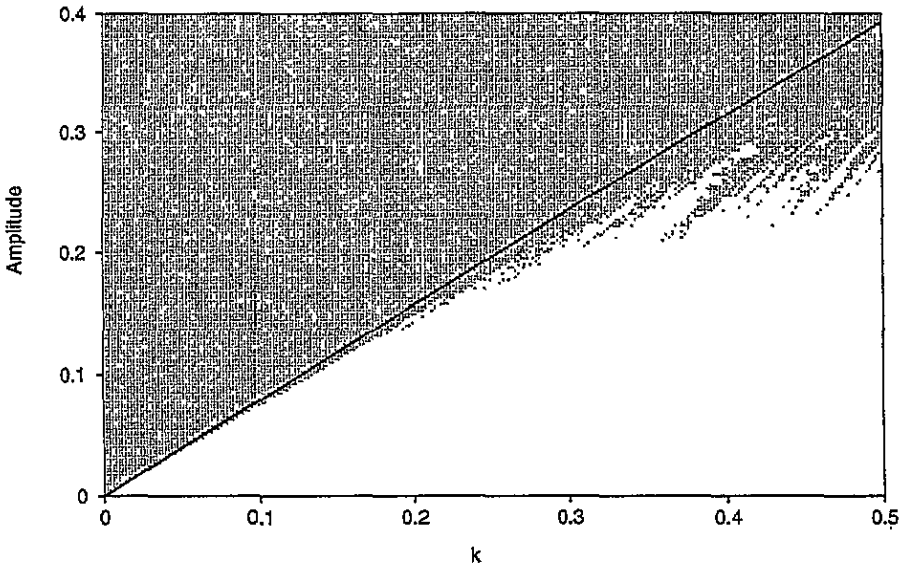


Figure 4. The boundary which separates the gap region (grey) from the transmission region (white) by numerical calculation. The black line is the long-wave-approximation prediction by equation (11). Parameters are the same as in figure 1.

4.3. The general non-linear case

Similarly, for the GNL model, the low-intensity wave equation becomes

$$\ddot{\psi} = - \left(k^2 - \frac{\lambda}{d} (\alpha_0 + \alpha_1 |\psi|^2) \right) \psi.$$

For a solution of the type of $\psi(n) = \psi_0 \exp[i\sigma n]$, we find

$$\sigma^2 = k^2 - \alpha_0 \frac{\lambda}{d} - \alpha_1 \frac{\lambda}{d} |\psi_0|^2.$$

Generally, transmission would be more difficult for small k because of the presence of the linear term, and it will get worse if $\alpha_1 > 0$. Compared with the corresponding linear model, better transmission would be achieved for small wavenumber k if the non-linear term dominates over the linear term, $\alpha_1 \gg \alpha_0$.

5. Concluding remarks

The main result that we have shown in the present work is related to the enhancement at low wave intensities of the propagating properties of a spatially quasiperiodic Kronig–Penney-type model when non-linearity is added to the model. Non-linearity in the form contained in equation (1) is shown to assist the waves in defying the quasi-random properties of the medium. This effect seems also to be present in genuine non-linear and disorder segments but with some differences [21]. The non-linear lattice model we have presented here has applications in the propagation of electrons in superlattices and electromagnetic waves in dielectric materials. Although we have shown here explicitly only the results for positive potentials ($\lambda > 0$ in equation (1)), it is worthwhile to mention that similar results exist for negative potentials with respect to the enhancement of long waves with small intensity by non-linearity. In the case of electromagnetic waves, equation (1) should be replaced

by a static Helmholtz equation, and similar but not identical transmission structures can be studied [15].

Acknowledgments

We acknowledge partial support from TARP grant number 003656-073c.

References

- [1] Colvard C, Merlin R, Klein M V and Gossard A C 1980 *Phys. Rev. Lett.* **45** 298
- [2] Camley R E, Rahman T S and Mills D L 1983 *Phys. Rev. B* **27** 261
- [3] Albuquerque E L and Cottam M G 1993 *Phys. Rep.* **233** 68 and references therein
- [4] Gellermann W, Kohmoto M, Sutherland B and Taylor P C 1994 *Phys. Rev. Lett.* **72** 633
- [5] Yablonovitch E 1987 *Phys. Rev. Lett.* **58** 2059
- [6] John S and Rangarajan R 1988 *Phys. Rev. B* **38** 10 101
- [7] Ho K M, Chan C T and Soukoulis C M 1990 *Phys. Rev. Lett.* **65** 3152
- [8] Sigalas M, Soukoulis C M, Economou E N, Chan C T and Ho K M 1993 *Phys. Rev. B* **48** 121
- [9] Chen W and Mills D L 1987 *Phys. Rev. Lett.* **58** 160
- [10] Yablonovitch E 1994 *J. Mod. Opt.* **41** 173
- [11] Hawrylak P, Grabowski M and Wilson P 1989 *Phys. Rev. B* **40** 6398
- [12] Grabowski M and Hawrylak P 1990 *Phys. Rev. B* **41** 5783
- [13] Johansson M and Riklund R 1994 *Phys. Rev. B* **49** 6587
- [14] Hennig D, Tsironis G P, Molina M and Gabriel H 1994 *Phys. Lett. A* at press
- [15] Hennig D, Gabriel H, Tsironis G P and Molina M I 1994 *Appl. Phys. Lett.* **64** 2934
- [16] Molina M I, Deering W D and Tsironis G P 1993 *Physica* **66D** 135
- [17] D. Würtz, Soerensen M P and Schneider T 1988 *Helv. Phys. Acta* **61** 345
- [18] Bellisard J, Formoso A, Lima R and Testard D 1982 *Phys. Rev. B* **26** 3024
- [19] Kohmoto M, Kadanoff L P and Tang C 1983 *Phys. Rev. Lett.* **50** 1870
- [20] Delyon F, Lévy Y-E and Souillard B 1994 *Phys. Rev. Lett.* **57** 2010
- [21] Molina M I and Tsironis G P 1994 *Phys. Rev. Lett.* to be published